Video Article

Preparation of Aligned Steel Fiber Reinforced Cementitious Composite and Its Flexural Behavior

Ru Mu[1], Luansu Wei[1], Xiaowei Wang[1], Hui Li[1], Longbang Qing[1], Jian Zhou[1], Quanming Zhao[2]

[1]School of Civil and Transportation Engineering, Hebei University of Technology

[2]School of Information Engineering, Hebei University of Technology

Correspondence to: Longbang Qing at qing@hebut.edu.cn

URL: https://www.jove.com/video/56307
DOI: doi:10.3791/56307

Keywords: Engineering, Issue 136, Steel fiber reinforced concrete, aligned steel fibers, cementitious composites, electromagnetic field, toughness, flexural strength, fiber distribution, orientation efficiency factor, mortar

Date Published: 6/27/2018

Citation: Mu, R., Wei, L., Wang, X., Li, H., Qing, L., Zhou, J., Zhao, Q. Preparation of Aligned Steel Fiber Reinforced Cementitious Composite and Its Flexural Behavior. *J. Vis. Exp.* (136), e56307, doi:10.3791/56307 (2018).

Abstract

The aim of this work is to present an approach, inspired by the way in which a compass needle maintains a consistent orientation under the action of the Earth's magnetic field, for manufacturing a cementitious composite reinforced with aligned steel fibers. Aligned steel fiber reinforced cementitious composites (ASFRC) were prepared by applying a uniform electromagnetic field to fresh mortar containing short steel fibers, whereby the short steel fibers were driven to rotate in alignment with the magnetic field. The degree of alignment of steel fibers in hardened ASFRC was assessed both by counting steel fibers in fractured cross-sections and by X-ray computed tomography analysis. The results from the two methods show that the steel fibers in ASFRC were highly aligned while the steel fibers in non-magnetically treated composites were randomly distributed. The aligned steel fibers had a much higher reinforcing efficiency, and the composites, therefore, exhibited significantly enhanced flexural strength and toughness. The ASFRC is thus superior to SFRC in that it can withstand greater tensile stress and more effectively resist cracking.

Video Link

The video component of this article can be found at https://www.jove.com/video/56307/

Introduction

Incorporating steel fibers into concrete is an effective way to overcome the inherent weakness of brittleness and to improve the tensile strength of concrete[1]. During the past decades, steel fiber reinforced concrete has been extensively investigated and widely used in the field. Steel fiber reinforced concrete is superior to concrete in terms of cracking resistance, tensile strength, fracture toughness, fracture energy, *etc.*[2] In steel fiber reinforced concrete, steel fibers are randomly dispersed, thereby uniformly dispersing the reinforcing efficiency of the fibers in every direction. However, under certain loading conditions, only some of the steel fibers in concrete contribute to the performance of the structural elements because the reinforcing efficiency of the fibers requires that they be aligned with the principle tensile stresses in the structure. For instance, when using steel fiber reinforced concrete containing randomly distributed steel fibers to prepare a beam, some of the steel fibers, especially those parallel to the direction of the principal tensile stress, will make major contribution to reinforcing efficiency, while those perpendicular to the direction of the principal tensile stress will make no contribution to reinforcing efficiency. Consequently, finding an approach to align the steel fibers with the direction of the principal tensile stress in concrete is necessary to achieve the highest reinforcing efficiency of the steel fibers.

The orientation efficiency factor, defined as the ratio of the projected length along the direction of the tensile stress to the actual length of fibers, is usually used to indicate the efficiency of the reinforcement of steel fibers[3,4]. According to this definition, the orientation efficiency factor of the fibers aligned with the direction of the tensile stress is 1.0; that of the fibers that are perpendicular to the tensile stress is 0. Inclined fibers have an orientation efficiency factor between 0 and 1.0. The analytical results show that the orientation efficiency factor of randomly distributed steel fibers in concrete is 0.405[4], while that from tests of ordinary steel fiber reinforced concrete is in the range of 0.167 to 0.500[5,6]. Evidently, if all the short steel fibers in concrete are aligned and have the same orientation as the tensile stress, the steel fibers will have the highest reinforcing efficiency and the specimens will have the optimum tensile behavior.

Some successful attempts to prepare aligned steel fiber reinforced concrete have been conducted since 1980s. In 1984, Shen[7] applied an electromagnetic field to the bottom layer of steel fiber reinforced cementitious composite (SFRC) beams during casting, and X-ray detection analysis revealed that steel fibers were well aligned. In 1995, Bayer[8] and Arman[9] patented the approach for preparing aligned steel fiber reinforced concrete using a magnetic field. Yamamoto *et al.*[10] considered the orientation of steel fibers in concrete to be mainly influenced by the casting approach and attempted to obtain aligned steel fiber reinforced concrete by keeping fresh concrete flowing into the formwork from a constant direction. Xu[11] attempted to align steel fibers in shotcrete by spraying steel fibers from a constant direction. Rotondo and Wiener[12] sought to make concrete poles with aligned long steel fibers by centrifugal casting. These experimental studies reveal that aligned steel fiber reinforced concrete has significant advantages over randomly distributed steel fiber reinforced concrete.

Recently, Michels *et al.*[13] and Mu *et al.*[14] have successfully developed a group of aligned steel fiber reinforced cementitious composites (ASFRCs) using electromagnetic fields. In these studies, various solenoids were made to provide a uniform magnetic field for aligning steel fibers in mortar specimens of different sizes. The solenoid has a hollow cuboid chamber, which can accommodate specimens of predefined sizes. When the solenoid is connected to direct current (DC), a uniform magnetic field is created in the chamber with a fixed orientation, which aligns with the axis of the solenoid. According to the principle of electromagnetics[15], magnetic fields can drive ferromagnetic fibers to rotate and align in fresh mortar. Appropriate workability of the mortar is critical for allowing steel fibers to rotate in fresh mortar. A high viscosity may cause difficulty in the alignment of the steel fibers in the mortar, while low viscosity may lead to the segregation of fibers.

This paper describes the details of the preparation of ASFRC specimens and tests the flexural properties of ASFRC and SFRC. It is expected that ASFRC has a higher flexural strength and toughness than SFRC. Thus, ASFRC potentially has advantages over SFRC in withstanding tensile stress and resisting cracking if used as cover concrete, pavement, *etc.*

Using the fractured specimens after flexural tests, the orientation of the steel fibers in the specimens is investigated by observing the fractured cross sections and utilizing X-ray scanning computed tomography analysis[16,17,18]. The mechanical properties of ASFRCs, including their flexural strength and toughness, are reported and compared with those of non-electromagnetically treated SFRCs.

Protocol

1. Solenoid Magnetic Field Setup

NOTE: The magnetic field is generated by a solenoid with a hollow chamber. The setup is a polybutylene terephthalate (PBT) board solenoid skeleton coiled with 4-6 layers of enamel insulated copper wire and wrapped with a plastic insulating layer for protection (**Figure 1**). After connecting the coil to DC, the current in the coil creates a uniform electromagnetic field within the solenoid chamber with a fixed direction and constant magnetic induction intensity. Use the magnetic field to align steel fibers in fresh mortar and prepare the ASFRC specimens. In this study, we prepared 150×150×550 mm prism specimens using a solenoid with a chamber size of 250×250×750 mm.

1. Correlate the magnetic induction intensity to the electrical current of the solenoid.
    1. Connect the solenoid to DC and apply current from 0 to 10 A with a step length of 1 A. Measure and record the magnetic induction intensity in the solenoid chamber using a tesla meter.
    2. Plot the magnetic induction intensity-current curve (**Figure 2**), which will be used in later steps to determine the necessary current of the solenoid.
    NOTE: Carefully follow electrical safety procedures when connecting the solenoid to the power source and in all other operation procedures relevant to electrical power.

2. Workability of Fresh Mortar

1. Prepare three mortar mixes with steel fiber volume fractions 0.8%, 1.2%, and 2.0%, respectively (**Table 1**). The three mixes have the same matrix composition with a water to cement to sand ratio of 0.42:1:2. According to the mix ratio, weigh 0.5 kg of cement, 1.0 kg of sand, and 0.21 kg of water for workability tests.
2. Add water to the mortar mixer first. Then add the cement. Mix the water and cement for 30 s. Then mix for another 30 s, and during this 30 s of mixing, gradually add sand to the mixer. Then mix for another 60 s.
3. Test the sinking depth of the mixture using a sinking depth meter following the Chinese standard for test method of performance on building mortar (JGJ/T70-2009)[19].
4. Repeat steps 2.2 and 2.3, adjusting the dosage of the superplasticizer until the sinking depth falls into the 50-100 mm range. Record the dosage of the superplasticizer that produces the desired workability and supplement it as part of the mix proportion in **Table 1**. Also test the specific density of the fresh mortar after the workability is achieved. The optimized dosage of a polycarboxylate superplasticizer from the aforementioned tests is 0.10% (mass ratio to cement), and the specific density of fresh mortar is 2186 kg/m^3.
5. Test the viscosity of the fresh mortar using a co-axial rotational mortar rheometer (**Figure 3**). The rheometer has a water bath that can maintain the temperature of the sample container at 20 °C.
    1. Put 300 mL of fresh mortar mixed within the previous 5 min into the sample container.
    2. Begin the viscosity test. The probe gradually drops into the fresh mortar in the container, and the container begins to rotate. As the fresh mortar moves within the rotating container, it applies a shear force on the probe. In the process, the rheometer records the shear stress and shear rate and plots the curve of shear stress to shear rate. The slope of the curve is the viscosity of the mortar[20,21]. In this investigation, the viscosity of the fresh mortar from tests is 0.82 Pas.

3. Specimen Preparation

1. Determine the magnetic induction intensity of the magnetic field and the current of the solenoid.
    1. Using the viscosity of the cement mortar determined in step 2.5.2, calculate the magnetic induction intensity of the magnetic field required for aligning steel fibers in cement mortar using Equation (1):[13]

$$B^2 = \frac{m^2 l_f \mu \mu_0}{12\pi r_f^2(\mu-1)(m-16\Delta t\eta\pi r_f)} \cdot \alpha(t+\Delta t) \quad (1)$$

    where B is magnetic induction intensity, η is the viscosity of fresh mortar, l_f is the length of steel fiber, m is the mass of an individual steel fiber, r_f is the radius of steel fibers, μ is the permeability of steel fibers, μ_0 is the permeability of the vacuum, Δt is time interval, and

$\alpha(t+\Delta t)$ is the angular acceleration at the next time interval. According to the viscosity and the parameters of the steel fiber used in the tests, the required magnetic induction intensity is 9.83 mT.

2. Determine the electrical current of the solenoid required to create a sufficient magnetic induction intensity according to **Figure 2** or Equation (2):[14]

$$I = \frac{B}{\mu_0 \cdot (N/L)} \quad (2)$$

where I is the required current, N is the number of solenoid turns, and L is the length of the solenoid.
Using Equation (2), the required current is 8.3 A, while from **Figure 2** it is about 8.5 A.

2. Prepare ASFRC specimens
    1. Use a 15 L mortar mixer to mix fresh mortar. For each batch, mix 7.5 L of mortar according to the mix proportions listed in **Table 1**. Table 1 denotes the ASFRC mixes as A-V_f, where A indicates that the steel fibers are aligned and V_f indicates the volume fraction of steel fiber. Accordingly, the SFRC mixes are denoted, for comparison, as R-V_f, where R indicates that the steel fibers are randomly distributed. The SFRC mixes are not listed in **Table 1** but have the same proportions as ASFRC.
    2. Weigh the raw materials and mix the steel fiber reinforced cement mortar following routine procedures.
    3. Pour the fresh mortar into a plastic mold with clear size of 150×150×550 mm. Cast the specimens promptly after mixing to avoid losing workability. It takes around 25 min to cast one ASFRC prism from the contact between cement and water.
    4. Move the mold onto a compacting table, and switch on the compacting table for 30 s. Add more mortar as needed to ensure that that the mold is completely filled.
    5. Put the mold into the chamber of the solenoid.
    6. Switch on the solenoid and compacting table for 50 s.
    NOTE: For ordinary concrete the reasonable compacting time is around 60-120 s. In this test, it is attempted to control the total compacting time within this range. Longer compacting time may improve the alignment of steel fibers; however, it may cause over compacting and consequently the segregation (the sinking of steel fibers and coarse aggregates if there are). Less compacting time may cause poor alignment of steel fiber and unconsolidated concrete.
    7. Switch off the compacting table.
    8. Switch off the solenoid after the compacting table has stopped completely.
    9. Gently take out the mold from the solenoid and smooth the top surface of the mortar with a trowel. Avoid disturbing the steel fibers near the top surface.

3. For each mix, prepare three electromagnetically treated specimens (following steps 3.2.2-3.2.9) and three non-electromagnetically treated specimens (following steps 3.2.2-3.2.4 and 3.2.9). In the preparation of non-electromagnetically treated specimens, the total compacting time was 80 s—the same as that in the preparation of electromagnetically treated specimens.
4. Leave the specimens indoors and in their molds for 24 h. Then demold and cure the specimens in a fog room until they are used for mechanical tests.

4. Three-Point Bending Test

1. After 28 days, take out the specimens from the curing room and mark the positions for loading (A), supports (B), mid-span deflection (C), and LVDT fixing points (D) (**Figure 4**).
2. Place the specimen on the three-point bending test rig (**Figure 4**) of the MTS test machine and fix a LVDT to the mid-span using a LVDT holder on each side surface of the specimen (**Figure 4**).
3. Connect the LVDT to a datalog. Then set the data acquisition frequency on the control PC of the test machine.
4. Gradually raise the specimen by raising the bottom supports so that the upper loading cell of the test machine is very close to, but not touching, the top surface of the specimen.
5. Zero the initial load, mid-span deflection (LVDT), and displacement (load cell) values.
6. Start the test and apply a three-point bending load to the specimen with a displacement control at a speed of 0.2 mm/min. Record the full history of the loading and mid-span deflection of the specimen.
7. Watch the load and deformation of the specimen. After peak value, when the displacement is greater than 30 mm, stop the test. Usually, the specimen is cracked and the load is less than 1.0 kN.
8. Repeat steps 4.1-4.7 to test all specimens.

5. Steel Fiber Orientation Analysis

1. Count the number of steel fibers on the fractured section.
    1. Separate the specimens into two portions at the cracked section.
    2. Measure and record the orientation of the steel fibers on the fractured cross section of the cement mortar specimen. The orientation is the angle between a steel fiber and the axis of the specimen. Because manually measuring the orientations of steel fibers is difficult and can produce inaccurate measurements, orientations can be categorized as one of six angle ranges: 0 - 15 °, 15 - 30 °, 30 - 45 °, 45 - 60 °, 60 - 75 ° and 75 - 90 °. Record the number of steel fibers in each group, and then calculate the average fiber orientation efficiency factor of the specimen using Equation (3):

$$\eta_\theta = \frac{\sum_1^n l_f \cdot \cos\theta_i}{n \cdot l_f} = \frac{1}{n}\sum_1^n \cos\theta_i \quad (3)$$

where η_θ is the average orientation efficiency factor of the steel fibers, l_f is the length of an individual steel fiber, n is the total number of steel fibers on the cracked section, and θ_i is the angle between a steel fiber and direction of the magnetic field applied to the specimen (in the calculation, the middle value of the angle range is adopted for all steel fibers in each group).

2. Perform X-ray computed tomography analysis.
    1. Cut a 75 mm cube from each mortar specimen.
    2. Perform the X-ray scanning of the cube using an X-ray computed tomography system. Place a specimen on the test platform and begin scanning. The specimen rotates 360 ° gradually and the machine records the attenuation of the X-rays caused by the specimen at each rotating step. The computed tomography system generates a three-dimensional digital structure of the cube.
    3. Identify the steel fibers in the digital cube structure by black and white binary processing. Then obtain the digital image describing the distribution of steel fibers.
    4. Determine the coordinates of all steel fibers by image analysis.
    5. Calculate the orientation of each steel fiber according to its coordinates.
    6. Calculate the orientation efficiency factor of the fibers using Equation (3).

Representative Results

The flexural strengths of ASFRCs and SFRCs determined from three-point bending tests are shown in **Figure 5**. The flexural strengths of ASFRCs are higher than those of SFRCs for all fiber dosages. The flexural strengths of ASFRCs were 88%, 71%, and 57% higher than those of SFRCs at the fiber volume fractions of 0.8%, 1.2%, and 2.0%, respectively. These results imply that the aligned steel fiber reinforces the cementitious matrix more effectively than randomly distributed steel fibers.

Figure 6 shows the load-deflection curves obtained from the three-point bending tests. The area under the load-deflection curve is defined as flexural toughness, which reflects the ability of energy absorption or consummation of the specimen when fractured. The toughness of ASFRCs and SFRCs was calculated and the results are given in **Table 2**. Like flexural strength, the toughness of ASFRCs was higher than that of SFRCs. The toughness values of ASFRCs were 48%, 77%, and 39% higher than those of SFRCs at the fiber volume fractions of 0.8%, 1.2%, and 2.0%, respectively.

Table 3 shows the distribution of steel fiber orientations determined after measuring the angle of fibers on fractured sections. The ASFRC specimens have much more fibers in the 0-15 ° angle range than in any other angle range. They also have more fibers in the 0-15 °angle range than the SFRC specimens. Thus, applying an electromagnetic field effectively controls the orientation of steel fibers. **Table 3** also shows that the total number of steel fibers on the fractured sections of the ASFRC specimens is greater than that of the SFRC specimens, which implies that ASFRC specimens have more steel fibers bridging the cracks than SFRC specimens. This difference may be the result of some of the fibers in the SFRC specimens being close and parallel to the fractured section; however, these steel fibers were not visible during inspection. **Table 3** also gives the orientation efficiency factors of steel fibers calculated according to the distribution of steel fiber orientations determined in the tests. The results indicate that the orientation efficiency factors of all ASFRC specimens are greater than those of the SFRC specimens. The orientation efficiency factors for the ASFRC specimens A-0.8%, A-1.2%, and A-2.0% are 0.90, 0.94, and 0.95, respectively. For SFRC specimens, in contrast, the factors are 0.75, 0.75, and 0.78 for R-0.8%, R-1.2%, and R-2.0%, respectively.

As shown in **Video 1** for specimens A-0.8% and **Video 2** for R-0.8%, the X-ray scanning and computed tomography analysis produces three-dimensional images showing the distribution of steel fibers in the specimens. The images reveal that most of the steel fibers in the ASFRC specimens are effectively aligned and have the same or similar orientation, while those in the SFRC specimens have a random orientation. From the X-ray computed tomography test results, the coordinates of fibers in the specimen can be determined and the orientation efficiency factor of the fibers in the specimen can be calculated. As shown in **Table 4**, the orientation efficiency factors obtained from X-ray computed tomography are consistent with those determined by counting on cross sections.

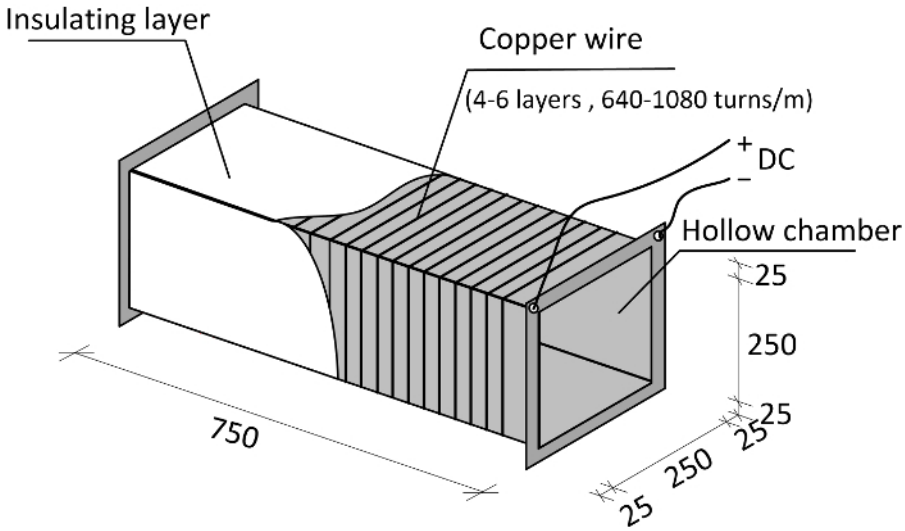

Figure 1. Solenoid magnetic setup. When connected to DC, a uniform magnetic field is created in the hollow chamber of the solenoid. This magnetic field is used to align steel fibers in cement mortar and prepare ASFRC specimens. Please click here to view a larger version of this figure.

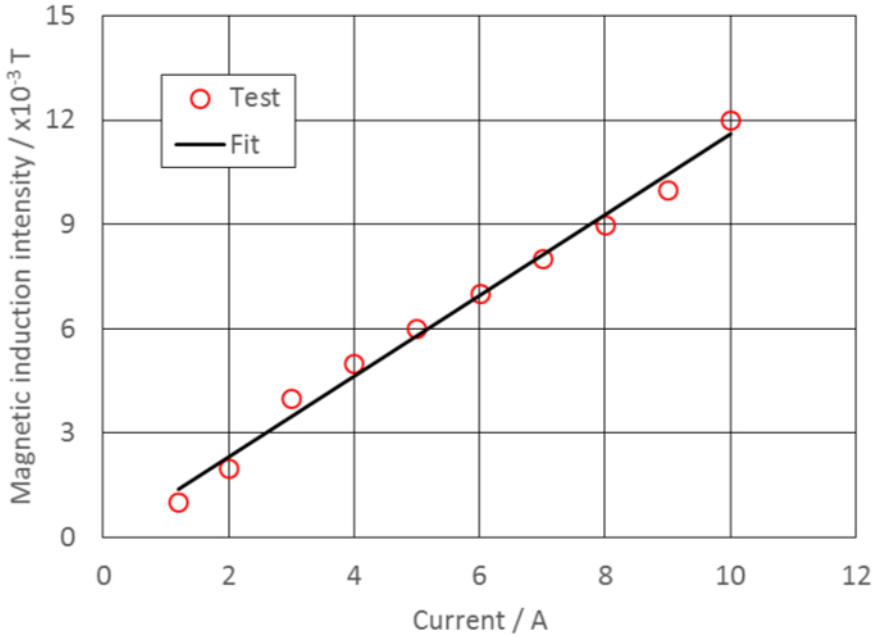

Figure 2. Magnetic induction intensity-current relationship. The relationship between magnetic induction intensity and current has been demonstrated through testing. This relationship is used to determine the current required to align steel fibers in fresh cement mortar. Please click here to view a larger version of this figure.

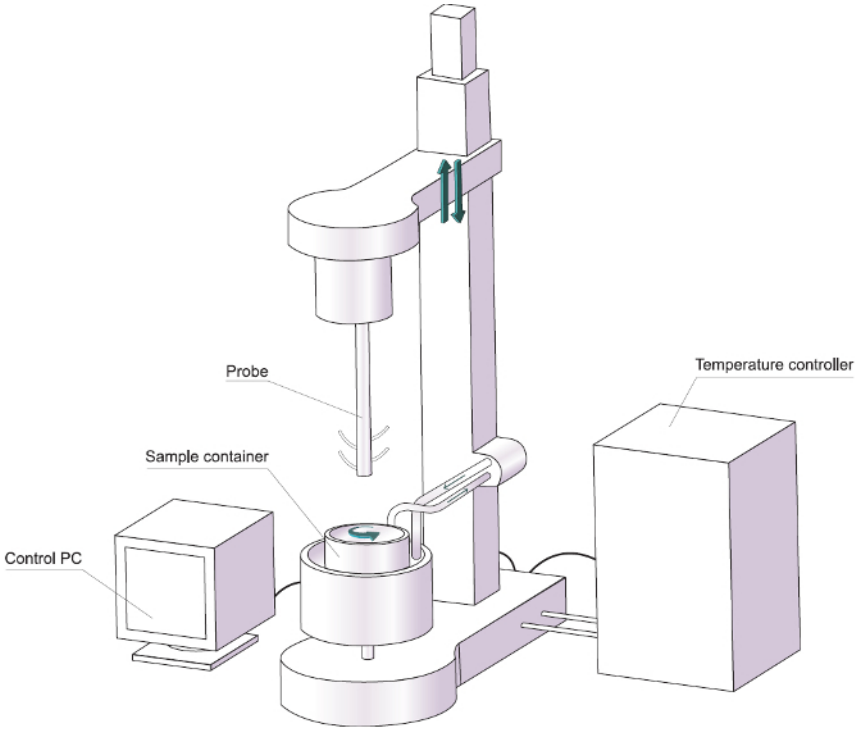

Figure 3. Rheometer setup. Using a rheometer, the relationship between shear stress and shear rate of fresh cement mortar is experimentally determined. The viscosity of the mortar can then be obtained. Please click here to view a larger version of this figure.

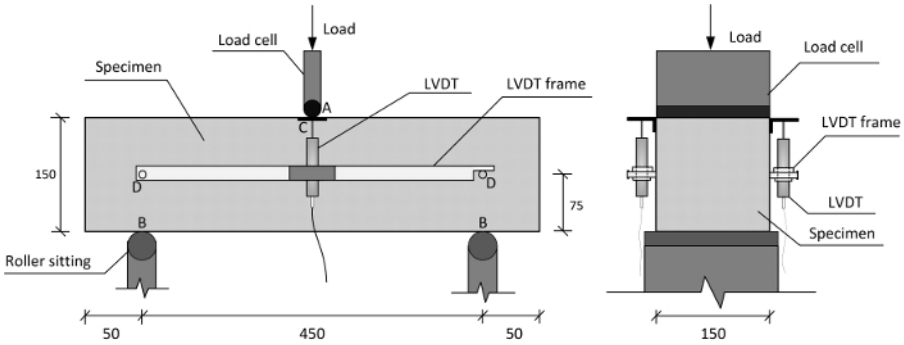

Figure 4. Loading specimen for three-point bending test. A three-point bending load is applied to the specimen with loading rate of 0.2 mm/min. The load and deflection are monitored. Please click here to view a larger version of this figure.

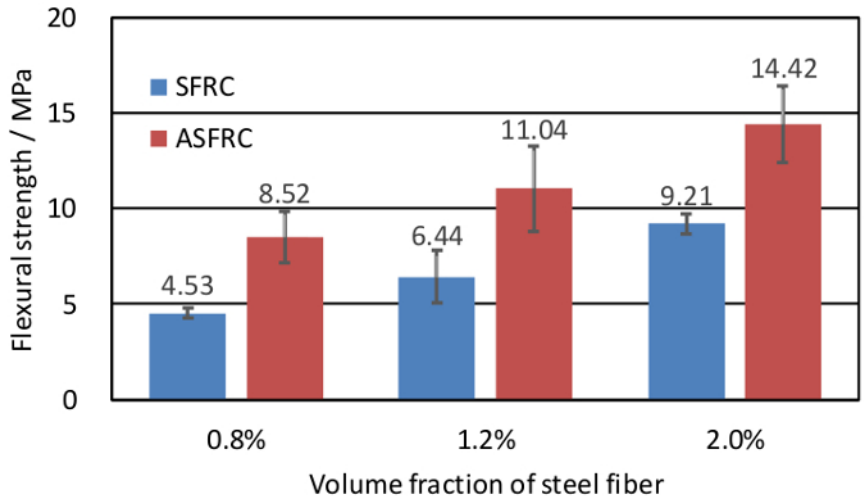

Figure 5. Flexural strength of ASFRCs and SFRCs. The flexural strength of each mix is the average of three samples. The error bars in the figure are standard deviation (SD) and indicate the dispersion of the tests. The results show that the flexural strength of ASFRC is higher than that of SFRC. Please click here to view a larger version of this figure.

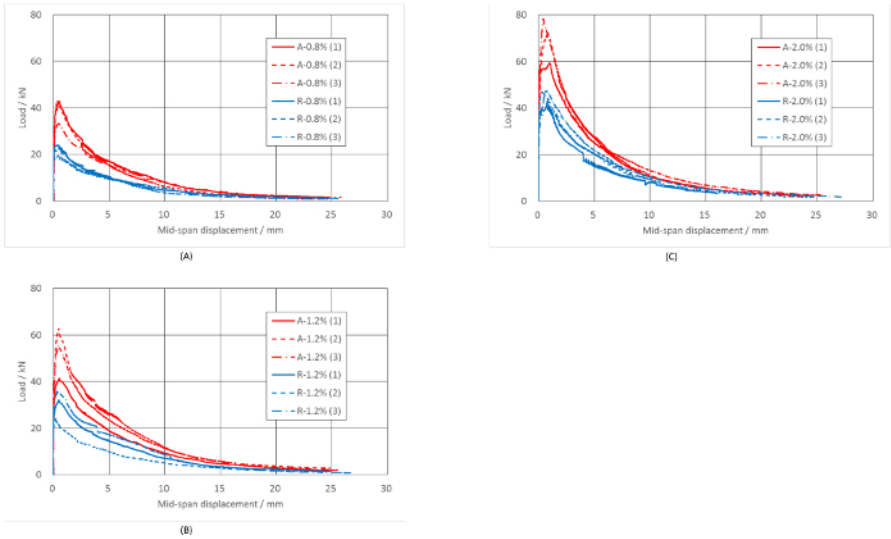

Figure 6. Load-deflection of ASFRC and SFRC specimens. (A) Volume fraction of steel fiber 0.8%, (B) Volume fraction of steel fiber 1.2%, (C) Volume fraction of steel fiber 2.0%. For each mix, three specimens are tested, and the three specimens are marked with a number in parentheses. The results show that ASFRC specimens have higher peak load and toughness values (the area under the curve) than SFRC specimens. Please click here to view a larger version of this figure.

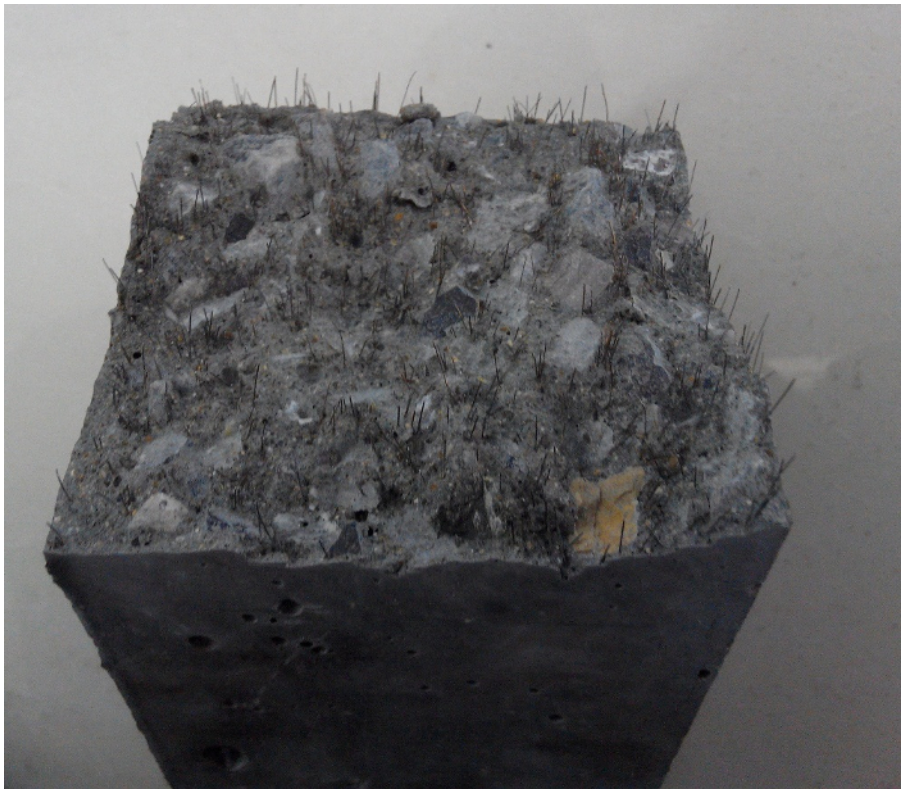

Figure 7. Aligned steel fibers on the fractured section of a steel fiber reinforced concrete sample. Although a number of coarse aggregates exist, the steel fibers in concrete are still effectively aligned. Please click here to view a larger version of this figure.

Video 1. Steel fiber distribution of A-0.8% from X-ray computed tomography tests. Results of X-ray computed tomography tests give the spatial distribution of steel fibers in the specimen and prove that the steel fibers in ASFRC specimens are highly aligned. Please click here to view this video. (Right-click to download.)

Video 2. Steel fiber distribution of R-0.8% from X-ray computed tomography tests. Results of X-ray computed tomography tests give the spatial distribution of steel fibers in the specimen and prove that the steel fibers in ASFRC specimens are highly aligned while those in SFRC specimens are randomly distributed. Please click here to view this video. (Right-click to download.)

Mix No.	Water (kg/m^3)	Cement (kg/m^3)	Sand (kg/m^3)	Steel Fiber (kg/m^3)	Superplasticizer (kg/m^3)
A-0.8%	267	633	1266	62.4	0.267
A-1.2%	265	631	1261	93.6	0.265
A-2.0%	263	627	1253	156.0	0.263

Table 1. Mix proportions of cementitious composites with aligned steel fiber reinforcement (ASFRC). The amount of the material in each line is for 1 m^3 composites. The SFRC counterparts have exactly the same proportions.

Specimen	**Toughness**	**Average toughness**	**Specimen**	**Toughness**	**Average toughness**
	(×10^{5}N•mm)	(×10^{5}N•mm)		(×10^{5}N•mm)	(×10^{5}N•mm)
A-0.8% (1)	2.047		R-0.8% (1)	1.495	
A-0.8% (2)	1.945	2.073	R-0.8% (2)	1.344	1.396
A-0.8% (3)	2.226		R-0.8% (3)	1.349	
A-1.2% (1)	2.323		R-1.2% (1)	1.738	
A-1.2% (2)	3.707	3.148	R-1.2% (2)	1.476	1.783
A-1.2% (3)	3.414		R-1.2% (3)	2.136	
A-2.0% (1)	3.125		R-2.0% (1)	1.692	
A-2.0% (2)	3.998	3.568	R-2.0% (2)	2.807	2.575
A-2.0% (3)	3.582		R-2.0% (3)	3.227	

Table 2. Toughness of ASFRC and SFRC specimens. The toughness of the specimen is the area under the load-deflection curve. The ASFRC specimens have higher values of toughness than the SFRC specimens.

Specimen	Number of fibers in angle range						Total	Orientation efficiency factor
	0-15 °	15-30 °	30-45 °	45-60 °	60-75 °	75-90 °		
A-0.8%	367	80	39	27	15	22	550	0.90
R-0.8%	133	102	83	67	49	45	479	0.75
A-1.2%	668	65	34	16	20	13	816	0.94
R-1.2%	142	120	98	72	61	41	534	0.75
A-2.0%	887	162	45	28	20	11	1153	0.95
R-2.0%	236	207	151	129	54	61	838	0.78

Table 3. Number of steel fibers on fractured mortar sections. The ASFRC specimens with aligned steel fibers have much more fibers in 0-15 °angle range than in any other angle range. They also have more fibers in 0-15 ° angle range than the SFRC specimens. The number of steel fiber was determined manually by counting the fibers on the fractured section of the specimens. The total number of steel fibers on the fractured sections of the ASFRC specimens is greater than that of the SFRC specimens.

	V_f=0.8%	**V_f=1.2%**	**V_f=2.0%**
ASFRC	0.91	0.93	0.94
SFRC	0.59	0.66	0.63

Table 4. Orientation efficiency factor of steel fibers in mortar from X-ray computed tomography analysis. The results from X-ray computed tomography analysis confirm that the steel fibers in the ASFRC specimens are effectively aligned and have higher orientation efficiency factors than the SFRC specimens.

Discussion

The electromagnetic solenoid developed in this study has a chamber measuring 250×250×750 mm and cannot accommodate the full size structural elements. Although the size of the chamber limits the application of the setup, the concept and protocol proposed in this paper will inspire the further development of a full size setup for manufacturing ASFRC elements, particularly precast elements.

Achieving an appropriate viscosity of fresh mortar is essential factor for controlling the quality of ASFRCs, because the alignment of steel fibers is driven by a magnetic force that needs to overcome the viscous resistance in the fresh mortar. The viscous resistance is governed by the viscosity of the fresh mortar. The lower the viscosity of the mortar, the easier it is to align steel fibers. On the other hand, the viscosity of the fresh mortar also influences the suspension of steel fibers. Very high viscosity of the fresh matrix leads to difficulty in aligning the steel fibers, while very low viscosity causes the segregation of steel fibers. Therefore, very high and very low viscosity reduce the efficiency of fiber reinforcement. Consequently, in order balance the alignment and suspension of the steel fibers, the viscosity of fresh mortar can be empirically controlled by ensuring that the sinking depth of fresh plain cement mortar remains in the 50-100 mm range.

Although the protocol described in this paper is used to prepare steel fiber reinforced cement mortar, it is also applicable to steel fiber reinforced concrete. Figure 7 is a photo of aligned steel fiber reinforced concrete with coarse aggregate prepared according to the protocol outlined above. For concrete, due to the presence of coarse aggregate, intuitively, the steel fibers are located in the gap between coarse aggregates and thus cannot be aligned. However, the trial test results show that the approach works well and that the steel fibers in concrete can be effectively aligned. In fact, in concrete, the volume fraction of coarse aggregate is roughly 35%; the other fine particles account for the remaining 65% volume fraction. This 65% volume provides ample space for the fiber to align. Therefore, this allows the proposed protocol has wider fields of application in both mortar and concrete.

In conclusion, 1) By using the solenoid electromagnetic field setup developed in this study, the steel fibers in fresh mortar were highly aligned and ASFRC specimens with maximum size of 150×150×550 mm were successfully prepared. 2) The orientation efficiency factors of steel fibers in ASFRC specimens exceeded 0.90, while those of SFRC specimens were around 0.60. In addition, the number of steel fibers bridging the cracked sections of the ASFRC specimens was greater than that of the SFRC specimens. Higher orientation efficiency factors and more steel fibers across cracked sections account for the increase in reinforcing efficiency of ASFRC. 3) The flexural strength and flexural toughness of ASFRC are significantly higher than those of SFRC at the fiber volume fractions of 0.8%, 1.2%, and 2.0%. Finally, 4) Though the protocol described in this paper was used to prepare steel fiber reinforced cement mortar, it is also applicable to steel fiber reinforced concrete. The proposed protocol therefore has wider fields of application in both mortar and concrete.

Disclosures

The authors have nothing to disclose.

Acknowledgements

The authors gratefully acknowledge financial supports from the National Nature Science Foundation of China (Grant No. 51578208), Hebei Provincial Nature Science Foundation (Grant No. E2017202030 and E2014202178), and Key Project of University Science and Technology Research of Hebei Province (Grant No. ZD2015028).

References

1. Zollo, R. F. Fiber-reinforced concrete: an overview after 30 years of development. *Cem. Concr. Compos.* **19** (2), 107 - 122 (1997).
2. Bentur, A., Mindess, S. *Fiber reinforced cementitious composites (2nd Edition).* Taylor & Francis, London and New York, (2014).
3. Deeb, R., Karihaloo B. L., Kulasegaram S. Reorientation of short steel fibres during the flow of self-compacting concrete mix and determination of the fiber orientation factor. *Cem. Concr. Res.* **56** (1), 112 - 120 (2013).
4. Soroushian, P., Lee, C. D. Distribution and orientation of fibers in steel fiber reinforced concrete. *ACI Mater. J.* **87** (5), 433 - 439 (1990).
5. Sebaibi, N., Benzerzour, M., Abriak, N. E. Influence of the distribution and orientation of fibres in a reinforced concrete with waste fibers and powders. *Constr. Build. Mater.* **65** (1), 254 - 263 (2014).
6. Lee, C., Kim, H. Orientation factor and number of fibers at failure plane in ring-type steel fiber reinforced concrete. *Cem. Concr. Res.* **40** (5), 810 - 819 (2010).
7. Shen, R. Effect of compaction methods on fibre orientation, flexural strength and toughness of steel fiber reinforced concrete. *J. of the Chinese Ceramic Society.* **12** (1), 21 - 31 (1984).
8. Bayer, A. G. *Process for producing a prepreg with aligned short fibres.* DE 3641828 A1. 1988-06-16. (1988).
9. Arman, E. *Building material, especially concrete or mortar, contains magnetically or electrically aligned parallel fibers.* DE19750746A1. 1999-05-20. (1999).
10. Yamamoto, T., Gasawara, N., Ohashi, T. The construction method and directional dispersion of steel fiber reinforced concrete. *Advances in Science and Technology of Water Resource.* (4), 188 - 197 (1983).
11. Xu, X. A new type of steel fiber reinforced concrete. *Architecture Technology.* **20** (4), 240 - 241 (1993).
12. Rotondo, P. L., Weiner, K. H. Aligned steel fibers in concrete poles. *Con. Int.* **8** (12), 22 - 27 (1986).
13. Michels, J., Gams, M. Preliminary study on the influence of fibre orientation in fibre reinforced mortars. *Gradevinar.* **68** (8), 645 - 655 (2016).
14. Mu, R., Li, H., Qing, L., Lin, J., Zhao, Q. Aligning steel fibers in cement mortar using electro-magnetic field. *Constr. Build. Mater.* **131** (1), 309 - 316 (2017).
15. Jones, D. S. *The theory of electromagnetism.* Pergamon Press, Oxford-London-New York-Paris, (1964).
16. Liu, J., Li, C., Liu, J., Cui, G., Yang, Z. Study on 3D spatial distribution of steel fibers in fiber reinforced cementitious composites through micro-CT technique. *Constr. Build. Mater.* **48** (2), 656 - 661 (2013).
17. Schnell, J., Schladitz, K., Schuler, F. Direction analysis of fibres in concrete on basis of computed tomography. *Betonund Stahlbetonbau.* **105** (2), 72 - 77 (2010).
18. Wuest, J., Denarié, E., Brühwiler, E., Tamarit, L., Kocher, M., Gallucci, E. Tomography analysis of fiber distribution and orientation in ultra high-performance fiber reinforced composites with high fiber dosages. *Experimental Techniques.* **33** (5), 50 - 55 (2009).
19. *JGJ/T70-2009 Chinese standard for test method of performance on building mortar.* Beijing, China Architecture & Building Press. (2009).
20. Roussel, N. *Understanding the Rheology of Concrete.* Woodhead Publishing Limited, Cambridge, (2012).
21. Roussel, N. Steady and transient flow behaviour of fresh cement pastes. *Cem. Concr. Res.* **35** (9), 1656 - 1664 (2005).

